View Article Online
View Journal

Catalysis
Science &
Technology

Accepted Manuscript

This article can be cited before page numbers have been issued, to do this please use: Y. Sasson, J. Rathod, P. Sharma, A. P. Singh and P. -. Kumar, *Catal. Sci. Technol.*, 2018, DOI: 10.1039/C7CY02619F.

ROYAL SOCIETY OF CHEMISTRY

rsc.li/catalysis

View Article Online
DOI: 10.1039/C7CY02619F

Catalysis Science & Technology

ARTICLE

Ok Received 00th January 20xx,
Accepted 00th January 20xx

DOI: 10.1039/x0xx00000x

www.rsc.org/

Synthesis of Heterogeneous Ru(II)-1,2,3-Triazole catalyst supported over SBA-15: Application to the Transfer Hydrogen reaction and unusual highly selective 1,4-disbustituted traizole formation via Multicomponent Click Reaction

Priti Sharma#[a], Jayant Rathod#[c], A.P. Singh*[b], Pradeep Kumar*[c] and Yoel Sasson*[a]

In the present study we demonstrate a simple and efficient method for ligand formation and covalent anchoring to heterogeneous support via click reaction. The complex tris(triphenylphosphine)ruthenium(II) dichloride [$RuCl_2(PPh_3)_3$] anchored over the click modified ligand of SBA-15, forms a new highly efficient heterogeneous SBA-15-Tz-Ru(II)TPP catalyst. Solid state ^{13}C, ^{29}Si, & ^{31}P CP-MAS NMR spectra provide evidence for the formation of the heterogeneous catalyst. SBA-15-Tz-Ru(II)TPP catalyst was screened for the multi component click cycloaddition reaction in water medium as green solvent exhibited unusual and excellent selectivity for the formation of 1,4-disubstituted triazole product under mild reaction condition. In addition, SBA-15-Tz-Ru(II)TPP catalyst also catalyzed the hydrogen transfer reaction of various carbonyl compounds with excellent catalytic activity to give the corresponding alcohols. The heterogeneous catalyst can be recycled and reused several times (five) without the loss in reactivity.

Introduction

In recent years, the "click chemistry" reaction is growing exceptionally with enhanced attention of the world wide researcher due to its applications in various fields such as medicine[1], material and polymer[2]. The click chemistry is associated with several advantage, such as simple and mild reaction procedure, atom efficient, compatibility with broad range of functional groups.[3] Apart from extensive application of click chemistry in various fields, novel ligand design and modification via 1,2,3-triazole has added a new dimention in the area of coordiantion chemistry. In click chemistry high level of selectivity has been demonstrated exclusively either 1,4 or 1,5-substituted 1,2,3-triazole with excellent yields, with its further application as coordination ligands with a various metal complexes.[4] In a remarkable work, *S. Hecht et al.* utilized the click chemistry and its chelating ability for transition metal complex via coordination [Clickates based on 2,6-bis(1,2,3-triazol-4-yl)pyridines].[5] In addition, Sarkar and his co-workers designed and synthesised novel ligands via click reaction (1,2,3-triazole) for metal complexes coordination and spin crossover complexes.[6] Crowley *et, al.* documented a book chapter is the extension of the appricable light of *Click-Triazole* in coordination chemistry.[7] With the fact, that 1,2,3-triazole shows good capability with metal complexes in coordination chemistry due to its homogeneous nature, it suffers the drawback of recyclability. In our recent work we have shown that the substituted 1,2,3-triazole can replace the traditional ligand and coordinate with metal complex via nitrogen-donor ligands in an efficient way.[8] In same context, we tried to design a new ligand with a covalent attachment to the heterogeneous support in a single step via 1,2,3-traizole formation (click reaction) (Scheme 1,2). Further, in the field of heterogeneous catalysis,[9] precisely, mesoporous materials like SBA-15 are preferred candidates for functionalization due to their high hydrothermal stability, large pore size and thick walls**,** which can be easily functionalized using free hydroxyl group of mesoporous SBA-15 (scheme 2).[10]

In literature, copper catalyzed click reaction generally proceeds with two component reaction system using organic azide.[11] However the key component of click reaction, organic azides are prone to explode and highly hazardous in process of purification and isolation.[12] Some reports are available by following in-situ azides synthesis, but faces drawback of tedious procedure coupled with high temperature and long reaction time, which might lead to the side product formation (homo coupling) and 1,5-disubstituted 1,2,3-triazole.[13]

---

[a] *Casali Center of Applied Chemistry, Institute of Chemistry, The Hebrew University of Jerusalem, Jerusalem, Israel, Email:* ysasson@huji.ac.il
[b] *Catalysis Division, CSIR-National Chemical Laboratory, Dr. Homi Bhabha Road, Pune 411008, India. Email:* ap.singh@ncl.res.in
[c] *Division of Organic Chemistry, CSIR-National Chemical Laboratory, Dr. Homi Bhabha Road, Pune-411008, India. Email:* pk.tripathi@ncl.res.in
[d.#] *Equal Contribution*

Electronic Supplementary Information (ESI) available: [^{31}P NMR of catalyst SEM-EDX analysis, TEM images, TEM-EDX, XPS result, P XPS, ^{1}H NMR of Intermediate 4-phenyl-1H-1,2,3-triazole, ICP, HR-XPS, Analytical Data of multi component click cycloaddition products.

View Article Online
DOI: 10.1039/C7CY02619F

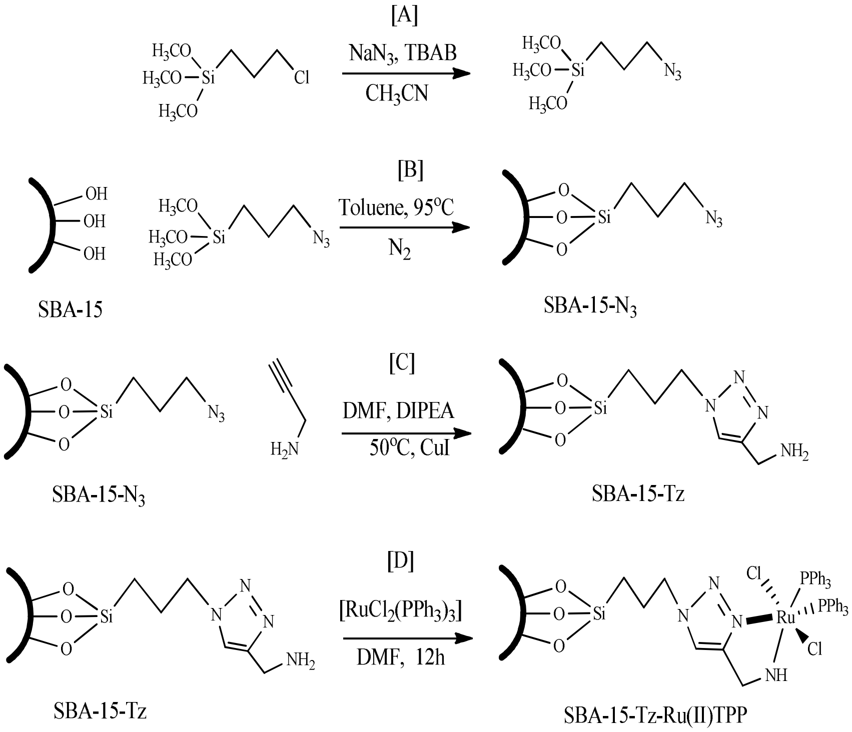

Scheme 1. Schematic diagram of; (A) 3-azidopropyltrimethoxysilane synthesis, (B) Azide-organo-functionalization over SBA-15, (C) SBA-15 ligand fabrication via 2-proprgylamine, and (D) $[RuCl_2(PPh_3)_3]$ complex anchoring over SBA-15-Tz**.**

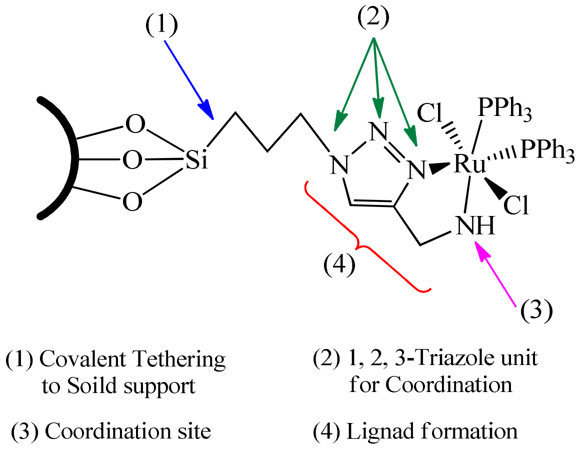

Scheme 2: Schematic representation of Click chemistry usage in ligand formation and covalent anchoring in an elementary step.

Recently apart from copper, many other metal[14] like ruthenium[15] complexes are reported, to catalyze the cycloaddition of terminal acetylenes and azides selectively to give 1,5 or 1,4-disubstituted triazole.[16] In a remarkable work; Liu and co-workers reported the catalyst dependent regioselective click reaction with the homogeneous cyclopentadienyl free ligands Ru-catalyst, for the selective formation of 1,4-disubstituted 1,2,3-triazole.[17] In the same context the present protocol here, multi-component, and selective 1,4-disubstituted 1,2,3-triazole regioselective product is achieved by using SBA-15-Tz-Ru(II)TPP heterogeneous catalyst. However the reaction sequence follows first the Ru-catalyzed cycloaddition of azide and alkyne to give the intermediate 4-phenyl-*1H*-1,2,3-triazole followed by sequential in-situ substitution reaction with benzyl bromide to give the 1,4-disubstituted 1,2,3-triazole compounds by homogenous $RuCl_2(PPh_3)_3$ complex and heterogeneous SBA-15-Tz-Ru(II)TPP catalyst (Scheme 3, 5.a, b, c).

Catalytic hydrogen transfer (CTH) reactions were developed as an alternative to the traditional catalytic hydrogenation processes and to avoid the processes, where hydrogen gas is used under pressure.[18], [19] The hydrogen transfer reaction has been performed employing catalyst such as homogenous catalyst[20], metal alloys[21], metal oxides[22] and organometallic complexes[23] on various solid supports[24] etc. But, ruthenium complex catalyzed reaction are most fundamental and favored with a broad coverage in hydrogen transfer reactions.[18d, 25] Although, reported processes generally progress in harsh reaction conditions and most of them are not recyclable. [26] For the best usage of homogeneous catalyst is to heterogenization over solid support.

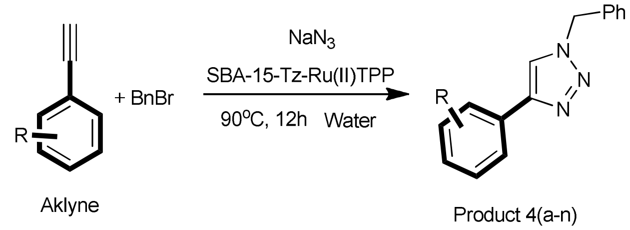

Scheme 3. Multi component click cycloaddition model reaction.

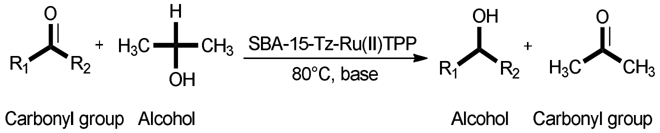

Scheme 4. Schematic diagram hydrogen transfer model reaction using carbonyl functional (>C=O) group and isopropanol.

Herein, we report a new heterogeneous catalyst, complexes $[RuCl_2(PPh_3)_3]$, over 1,4-substituted 1,2,3-triazole liganded SBA-15 (click modified) and screened its catalytic properties in

View Article Online
DOI: 10.1039/C7CY02619F

multi component click cycloaddition and hydrogen transfer reaction.

Results and discussion

The synthesis strategy employed to fabricate SBA-15-Tz-Ru(II)TPP heterogeneous catalysts is shown in scheme 1. As per scheme 1, free hydroxyl group of mesoporous SBA-15 heterogeneous support, is first covalently anchored by azido linker group (3-Az-PTMS), and then modified to triazole ligand via click reaction by propargylamine. Further, procedure involves stirring and refluxing a mixture of click functionalized SBA-15-Tz, with solution of [RuCl$_2$(PPh$_3$)$_3$] in DMF for 12 h under argon atmosphere. (Scheme 1).

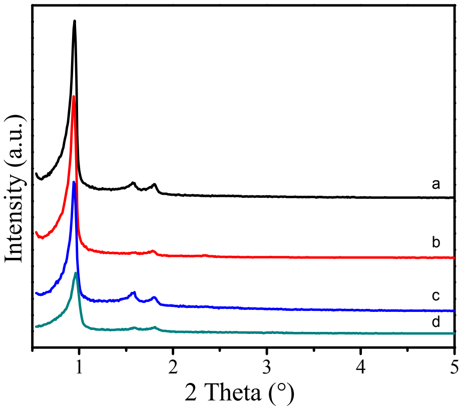

Figure 1. Small angle XRD patterns of; (a) SBA-15, (b) SBA-15-N$_3$, (c) SBA-15-Tz, (d) SBA-15-Tz-Ru(II)TPP.

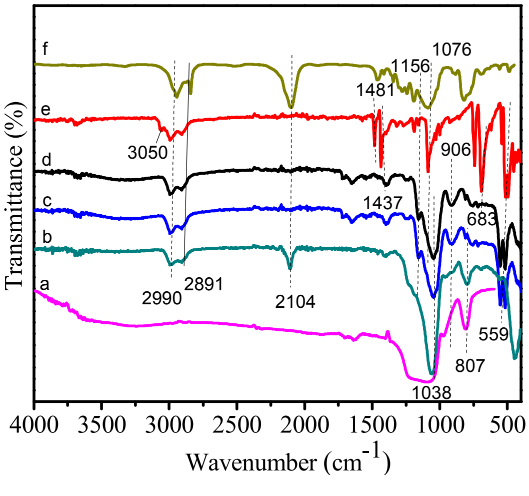

Figure 2. FT-IR spectra of; (a) Calcined SBA-15, (b) SBA-15-N$_3$, (c) SBA-15-Tz, (d) SBA-15-Tz-Ru(II)TPP, (e) RuCl$_2$(PPh$_3$)$_3$, (f) 3-Az-PTMS.

The synthesized catalysts were characterized by different physicochemical characterization techniques and the results are discussed here in detail. The XRD pattern of SBA-15 (a), SBA-15-N$_3$ (b), SBA-15-Tz (c) and SBA-15-Tz-Ru(II)TPP (d) are presented in figure 1. The observed X-ray diffraction pattern demonstrates characteristic highly ordered hexagonal mesoporous silica framework of the synthesized click modified materials (Fig.1).[27] The characteristic hexagonal phase (p6mm) of SBA-15 shows three reflection planes, intense peak at (100), peaks with low intensity (110) and (200) are visible in all modified SBA-15 materials at 2y = 0.949°, 1.565° and 1.799°, respectively. The observed results support high degree of orderedness of the two dimensional (2D) hexagonal phase (Fig.1a).[28] The peak intensities of reflections (100) in SBA-15-N$_3$, SBA-15-Tz and SBA-15-Tz-Ru(II)TPP are in decreasing order from calcined SBA-15 to modified SBA-15 material moderatly in figure 1 (a-d), due to surface modification and anchored organometallic complex, respectively, by using free clickable surface of SBA-15 (Fig. 1a-d).[29]

FTIR spectra witnesses the presence of surface silanols, hydroxyl group, anchored complex, RuCl$_2$(PPh$_3$)$_3$ in (a) Calcined SBA-15, (b) SBA-15-N$_3$, (c) SBA-15-Tz, (d) SBA-15-Tz Ru(II)TPP, (e) RuCl$_2$(PPh$_3$)$_3$, (f) 3-Az-PTMS, materials in figure 2. The strong visible bands in the range of 807–770 cm^{-1} and 1038-1090 cm^{-1} are accountable for symmetric and asymmetric stretching vibrations of the Si–O–Si bonds SBA-15, and modified SBA-15 materials respectively (Fig.2 a-d).[8, 27, 29] Further, a strong band is observed in the mid-infrared region at 906 cm^{-1}, attributed to the Si-OH vibrations (Fig.2 a-d). The FT-IR spectra of SBA-15-N$_3$, SBA-15-Tz and SBA-15-Tz-Ru(II)TPP materials, exhibit two bands at 2990 cm^{-1} and 2891 cm^{-1}, are asymmetric and symmetric vibrations of the -CH$_2$ groups of the linker propyl chain (3-azidopropyltrimethoxy silane) (Fig.2 b-d) respectively. Furthermore, SBA-15-N$_3$ shows a sharp absorbance at 2104 cm^{-1}, characteristic stretching vibration of organic azide (-N$_3$). The presence of similar absorption band visible in the pure homogeneous 3-azidopropyltrimehtoxysilane linkers (2104 cm^{-1}), proves successful anchoring of the linker to calcined SBA-15 (Fig.2 b,f).[30] Further, the complete consumption of above mentioned (-N$_3$, 2104 cm^{-1}) characteristic peak in SBA-15-Tz material, demonstrates that 3-azidopropyl tethering agent successfully reacted with propargylamine via click reaction (Fig. 2c). A strong characteristic vibration of PPh$_3$ (aromatic region) complex in FT-IR evidenced at 683, 700, 1076, 1437, 1481 and 3050 cm^{-1} in homogeneous catalyst, whereas with less intensity same vibration are visible in heterogeneous catalyst SBA-15-Tz-Ru(II)TPP, supports the fact that, PPh$_3$ group may leave the complex after anchoring (due to trans effect) (Fig. 2e and 2d).[31] The spectra of heterogenized complex SBA-15-Tz-Ru(II)TPP catalyst witnesses characteristic peaks of the neat catalyst, indicating the structural retention of [RuCl$_2$(PPh$_3$)$_3$] complex after immobilization.

The ^{13}C solid state CP MAS NMR spectra of (A) SBA-15-N$_3$, (B) SBA-15-Tz-Ru(II)TPP are depicted in figure 3. The presence of peaks at 10, 23 and 54 ppm are assigned to the carbon atoms of the linker propyl chain in azido (SBA-15-N$_3$) group, indicates covalent azido functionalization of SBA-15 (Fig. 3a). The appearance of additional intense peaks precisely in aromatic region of PPh$_3$ group from 117 to 138 ppm (consisting 127, 143, 144, 146) clearly demonstrate the functionalization of the

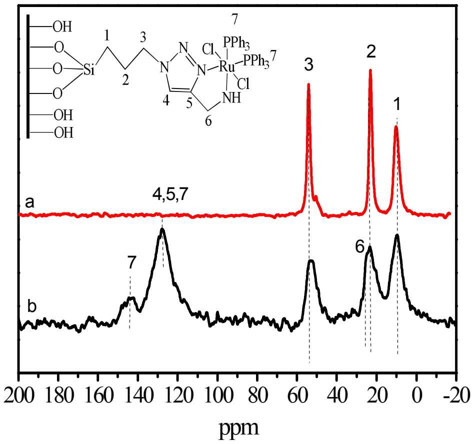

Figure 3. ^{13}C CP-MAS NMR of; (a) SBA-15-N_3, (b) SBA-15-Tz-Ru(II)TPP.

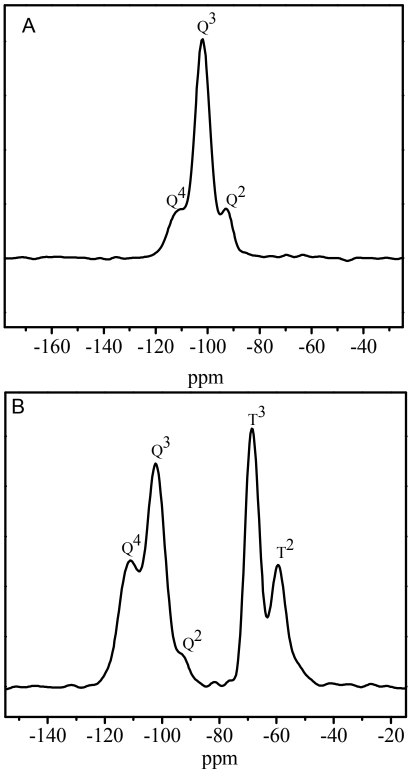

Figure 4. ^{29}Si CP-MAS NMR of: (A) calcined SBA-15, (B) SBA-15-Tz-Ru(II)TPP.

Ru(II)TPP complex over clickable SBA-15 support (Fig. 3b).[8, 30a, 32] These NMR results demonstrate the successful immobilization of [$RuCl_2(PPh_3)_3$] complex on the clickable surface of SBA-15 support.

The functionalization of free hydroxyl groups of SBA-15 with organic moiety could be accessed by ^{29}Si CP MAS NMR spectroscopy. Figure 4 (A,B) exhibit the ^{29}Si CP MAS NMR spectra of calcined SBA-15 and SBA-15-Tz-Ru(II)TPP catalyst. The spectrum exhibited in figure 4A broad resonance peaks from -90 to -120 ppm, is indicative for a range of Si–O–Si bond. While the bands centered at -93 ppm, -102 ppm and -111 ppm are assigned to Q^2 [$(SiO)_2Si(OH)_2$], Q^3 [$(SiO)_3Si(OH)$] and Q^4 [$(SiO)_4Si$] sites of the framework of SBA-15, respectively (Fig. 4 B). In general, the Q^3 sites are considered to be loaded with Si–OH groups. The Q^2 sites are frequently attainable for possible anchoring with organic complexes. ^{29}Si CP MAS NMR spectrum of SBA-15-Tz-Ru(II)TPP show two peaks at -67 ppm and at -60 ppm which are designated to T^3 [$SiR(OSi)_3$] and T^2 [$Si(OH)R(OSi)_2$], respectively (Fig. 4B).[27a, 29-30] The presence of sharp T^3 peak indicates the covalent anchoring of 3-azidopropyltrimethoxy silane over clickable mesoporous SBA-15 surface for further anchoring of complex (Fig. 4B) (SI, Fig. S7).

^{31}P CP MAS NMR spectrum of heterogeneous catalyst SBA-15-Tz-Ru(II)TPP exhibits two ^{31}P signals at d = 34, 50 ppm (Fig. S1). After interacting to click modified SBA-15 triazole ligand one equatorial PPh_3 group leaves from the $RuCl_2(PPh_3)_3$ homogeneous complexes system (due to strong trans effect of another PPh_3 group, two non-equivalent phosphorus environment).[31, 33] The spectrum represents two signals (d = 34, 50 ppm) of merging in one peak intensity, indicating the presence of two non-equivalent phosphorus atoms in the synthesized catalyst SBA-15-Tz-Ru(II)TPP (Fig. S1).

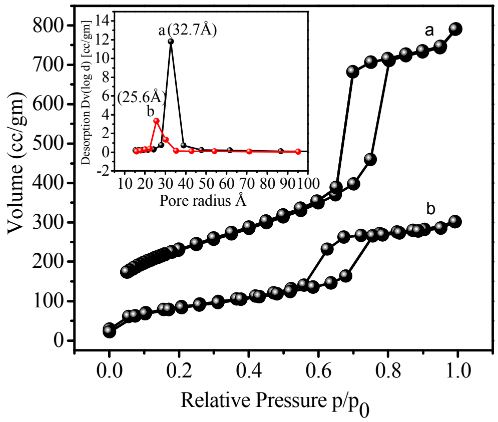

Figure 5. N_2 adsorption-desorption isotherm & Pore size distribution (inset) of: (a) calcined SBA-15, (b) catalyst SBA-15-Tz-Ru(II)TPP.

Table 1. Textural properties of SBA-15 & catalyst SBA-15-Tz-Ru(II)TPP.

	BET surface area (m^2/g)	**Average pore radius) (Å)**	**Pore volume (Vp, cm^3/g)**
SBA-15	830.7 m²/g	32.7 Å	1.13 cc/g
SBA-15-Tz-Ru(II)TPP	314.6 m²/g	25.696 Å	0.425 cc/g

View Article Online
DOI: 10.1039/C7CY02619F

The observed nitrogen adsorption desorption results of SBA-15, SBA-15-Tz-Ru(II)TPP with corresponding pore size distribution curves are plotted in figure 5 and details summarized in table 1. The surface area, average pore diameter and pore volume observed for SBA-15 and SBA-15-Tz-Ru(II)TPP catalyst are summarized in the table 1. Both synthesized materials SBA-15 and SBA-15-Tz-Ru(II)TPP exhibit type IV adsorption isotherms with a hysteresis characteristic for mesoporous materials with uniformly size, completely reversible nature, with a capillary condensation step at P/Po=0.3–0.4 (As per IUPAC classification). The total surface area, average pore radius and pore volume observed for SBA-15 and SBA-15-Tz-Ru(II)TPP, were observed 830 m^2g^{-1}, 32.7Å, 1.13 cm^3g^{-1} and 314 m^2g^{-1}, 25.7 Å, 0.425 cm^3g^{-1}, respectively. The noticeable change (decrease) in total mesoporous surface area (62%), pore radius (21%) and pore volume (53%) after tris(triphenylphosphine)ruthenium(II) dichloride $[RuCl_2(PPh_3)_3]$ immobilization over click modified SBA-15 is indicative of the successful immobilization of complex over the mesoporous SBA-15 (Table 1) and consistent with the XRD and XPS results (Figure 1, 5, 6).

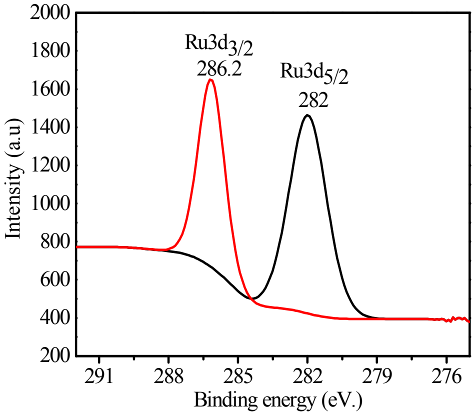

Figure 6. Ru XPS spectrum of SBA-15-Tz-Ru(II)TPP.

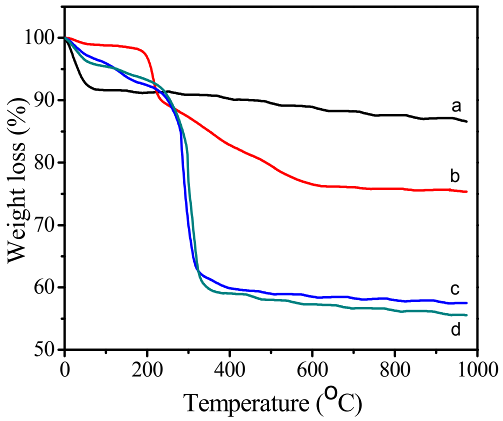

Figure 7. TGA analysis of: (a) Calcined SBA-15, (b) SBA-15-N_3, (c) SBA-15-Tz, (d) SBA-15-Tz-Ru(II)TPP.

The XPS spectrum of SBA-15-Tz-Ru(II)TPP is displayed in figure 6. The accuracy of the observed binding energy (B.E.) is ±0.3 eV. The Ru3d core level XPS spectrum shows two binding energy (B.E.) peaks centered at 282 eV and 286 eV, respectively. The first peak (282 eV) is well resolved and can be assigned to the BE of $Ru3d_{5/2}$. As the second peak (286 eV) is associated with the contribution $Ru3d_{3/2}$, the peak at 286 eV is deconvoluted and can be assigned to the existence of Ru in the +2 oxidation state in catalyst SBA-15-Tz-Ru(II)TPP (Fig. 6).[34] P XPS analysis value for the $2p_{3/2}$ and $2p_{1/2}$ core level are distinguished at 131.3 and 132.1 respectively (Fig. S5). The value for phosphorous (P) XPS in SBA-15-Tz-Ru(II)TPP is in good agreement with the literature value and confirms the $[RuCl_2(PPh_3)_3]$ complex retained when anchored over the organomodified support SBA-15 (Fig. S6).[31a]. For the clear aspects of Ru, P, Cl elements presence in SBA-15-Tz-Ru(II)TPP is confirmed by HR-XPS with complete spectrum (SI, Fig. S8).

The thermal behavior of all the synthesized materials (A) SBA-15, (B) SBA-15-N_3, (C) SBA-15-Tz, (D) SBA-15-Tz-Ru(II)TPP was studied by thermo gravimetric analysis (TGA), in air atmosphere, from temperature up to 1000°C with an increment of 10°C min^{-1} (Figure 7). The TGA plots of all click modified SBA-15 samples show nearly 6% weight loss below 120°C, due to the desorption of absorbed water molecules (Fig. 7,a-d). In the shown TGA plot, almost no weight loss was observed for the calcined SBA-15 material between 120°C and 200°C, indicates the complete discharge of surfactant from SBA-15 (Fig. 7a). The TGA results of the SBA-15-N_3 material show weight loss in two steps. In the first step, a weight loss between 70°C and 140°C corresponds to the loss of water

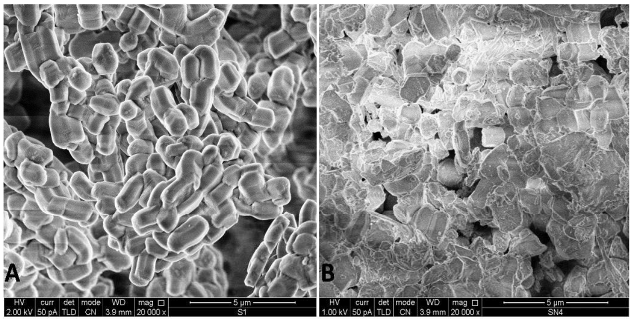

Figure 8. SEM images of (A) calcined SBA-15 and (B) SBA-15-Tz-Ru(II)TPP.

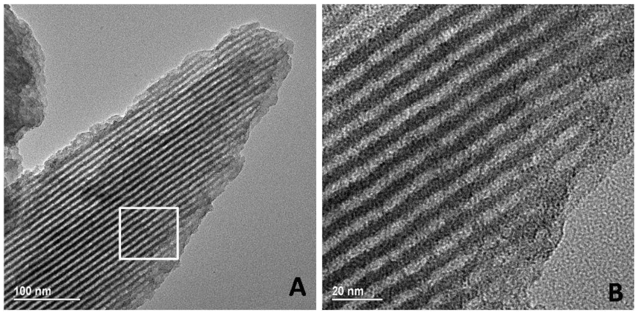

Figure 9. TEM images of SBA-15-Tz-Ru(II)TPP at different magnification at; (A) 100 nm , (B) 20 nm.

View Article Online
DOI: 10.1039/C7CY02619F

(adsorbed moisture). In the second step, a weight loss was observed in the range of 255°C–365°C; temperature regions (255–365°C) attributed to 3-Az-PTMS (Fig. 7b). The TGA plot of SBA-15-N_3 quantitatively shows the ~11.25% weight loss, which is greater than the calcined SBA-15, strongly supports the on track anchoring of the 3-Az-PTMS over SBA-15 (Fig. 7a,b). In the case of click modified triazole complex SBA-15–Tz, one extra step weight loss in range of 250°C to 350°C was observed along with existing weight losses shown in the SBA-15-N_3 (Fig.7.b,c). A categorical comparison of heterogenized SBA-15-Tz-Ru(II)TPP, and functionalized SBA-15-Tz in terms of weight loss shows an ~2 weight % loading of the complex material, results are in good agreement with XPS and ICP-OES results (Fig. 7a-d, Fig.S5, S9).

The SEM images of (A) SBA-15 and (B) SBA-15-Tz-Ru(II)TPP are shown in figure 8. The morphology of SBA-15-Tz-Ru(II)TPP was owned with the host mesoporous material SBA-15 after the anchoring of $[RuCl_2(PPh_3)_3]$ complex on azido functionalized SBA-15.[27a, 30a] The calcined SBA-15 shows cylindrical rod-like structure with wormlike morphology in the SEM images. Further, the SBA-15-Tz-Ru(II)TPP demonstrated to be alike molecular based material, the large molecular system changes into closely compacted together with respect to the SBA-15 after the $[RuCl_2(PPh_3)_3]$ complex is immobilized over the clickable mesoporous surface (Fig. 8 A,B). Moreover, the EDX pattern of SBA-15 and SBA-15-Tz-Ru(II)TPP indicates the presence of ruthenium in the synthesized heterogeneous catalyst SBA-15-Tz-Ru(II)TPP (Fig. S2).

The TEM images of the SBA-15 and SBA-15-Tz-Ru(II)TPP provide structural evidence that the material is organized into ordered arrays of two dimensional hexagonal mesopores and parallel channel structure with thick walls of the mesoporous materials clearly visualized with the different magnifications (Fig. 9 A,B, SI: S3). However, after the anchoring of the $[RuCl_2(PPh_3)_3]$ complex over the clickable mesoporous channels of SBA-15 the image show darker contrast meso parallel channels, in comparison to the SBA-15 surface, corresponds to the proper anchoring of $[RuCl_2(PPh_3)_3]$ complex over the clickable surface of the SBA-15 (Fig. 9 A,B).[27] EDX obtained from TEM analysis evidently confirms the presence of elemental ruthenium, phosphorous in the heterogeneous catalyst SBA-15-Tz-Ru(II)TPP (Fig. S4).

Catalytic Activity

Multicomponent Click Reaction

After thorough characterization, we proceeded further in screening of multi component click cycloaddition of alkyne, azide and alkyl halide (Scheme 3). This represents a powerful method for the 1,4-disubstituted 1,2,3-triazole formation compared to traditional click two component reaction. Extensive research have been done in multicomponent reaction, but only few of them are recyclable and need additives for enforced recycling viz; supported copper catalyst.[35] However, these catalytic system suffers from drawbacks, like use of additive, sodium ascorbate, and organic solvents like dioxane, acetonitrile for reactions.[36]. We began with optimising the multicomponant click reaction of phenyl acetylene, sodium azide and benzyl bromide using homogeneous Ru Catalyst with respect to solvent and ligands and compare the results with our synthesised heterogeneous Ru catalyst on the regioselectivity of the triazole formation (Table 2). As per literature precedence the click reaction using Ru as catalyst gives the 1,5-disubstituted triazole heterocycles. When the Cu salt is used as catalyst, it shows different selectivity and provides the 1,4-disubstituted triazols. There are only two reports for the Ru catalysed click reaction which show the contradicting result than the usual outcome for reaction with certain limitations. So considering this we hypothesized the multi componant click reaction of alkyne, sodium azide and benzyl bromide.

In order to optimize the reaction condition phenyl acetylene, sodium azide and benzyl bromide were slected as model substrate and screened with various Ru catalyst for the click reaction, We began with $RuCl_3$ as catalyst and PPh_3 as ligand using DMF as solvent at 90 °C the reaction ended up with the very poor yields and reverse selectivity (i.e. 1, 4 substituted triazole) (Table 2 entry 1). Further to optimize reaction conditions various solvents like DMSO, dioxane, toluene were tested but unfortunately there was little improvement with maximum yield up to 26 % (Table 2, entry 2-4). To our delight, when reaction was performed using water as solvent, the yield was increased up to 48% with reverse selectivity. To optimize the yield, the reaction was performed with different ligands such as DMAP and 2-amino-6-picoline but it ended up with lowering in the yield of product (Table 2. entry 6, 7). When the Ru catalyst was changed to $[Ru(p\text{-}cym)Cl]_2$ the improvement in the yield was not observed, We then considered the reaction in homogeneous conditions switching over to heterogeneous condition from the homogeneous. Accordingly when the reaction performed with organosilica supported Ru catalyst SBA-15-Tz-Ru(II)TPP , in water as solvent, and the reaction proceeded very smoothly with the excellent yield of desired product and with reverse selectivity (88%) (Table 2, entry 9).

We further proceeded to optimize the reaction condition with heterogeneous catalyst to establish a protocol in, water as a green solvent. Few of catalytic systems are active in aqueous solution, such as $CuSO_4$/copper ion complex[37] but, with high concentration of copper complex. At our hand, we optimised the multi component click reaction with respect to solvent, and temperature and the results are summarized in table 3 & 4.

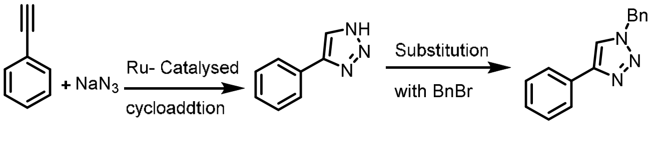

Scheme 5a. Intermediate 4-phenyl-*1H*-1,2,3-triazole formation

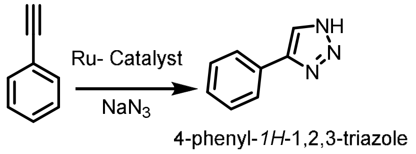

Scheme 5b. Intermediate 4-phenyl-*1H*-1,2,3-triazole formation via homogeneous Catalyst

View Article Online
DOI: 10.1039/C7CY02619F

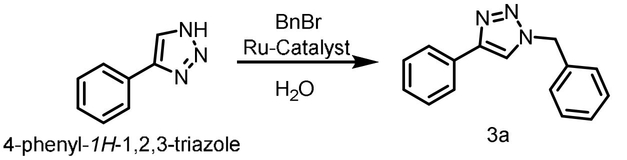

Scheme 5c. Intermediate 4-phenyl-*1H*-1,2,3-triazole reacts with BnBr

A variety of solvents, such as, DMSO, DMF, EtOH, t-BuOH, THF and water were screened, in the presence of SBA-15-Tz-Ru(II)TPP catalyst at 90 °C, in a model reaction of the multi component click cycloaddition between phenyl acetylene (1 mmol), benzyl bromide (1.2 mmol) and sodium azide (1.2 mmol) (Table 3). Solvents like DMSO, DMF, EtOH, t-BuOH THF were not able to give a significant yield (20-63%) even after 24 h reaction time period (Table 3, entries 1, 2, 3, 4, 5 and 8). In addition, the reaction was also carried out at room temperature using SBA-15-Tz-Ru(II)TPP catalyst in the presence of water and DMSO solvent under similar reaction conditions. But no progress of reaction was observed even after 24 h reaction period (Table 3, entries 1 and 7). The green solvent water was found to be the most suitable under the optimized reaction conditions (Table 3, entry 9). From the obtained results of the solvent optimization for the conversion of phenylacetylene, the reactivity order of solvents emerged as follows; water (88%) > DMF (63%) > EtOH (50%) > DMSO (46%) > t-BuOH (35%) > THF (20%), respectively.

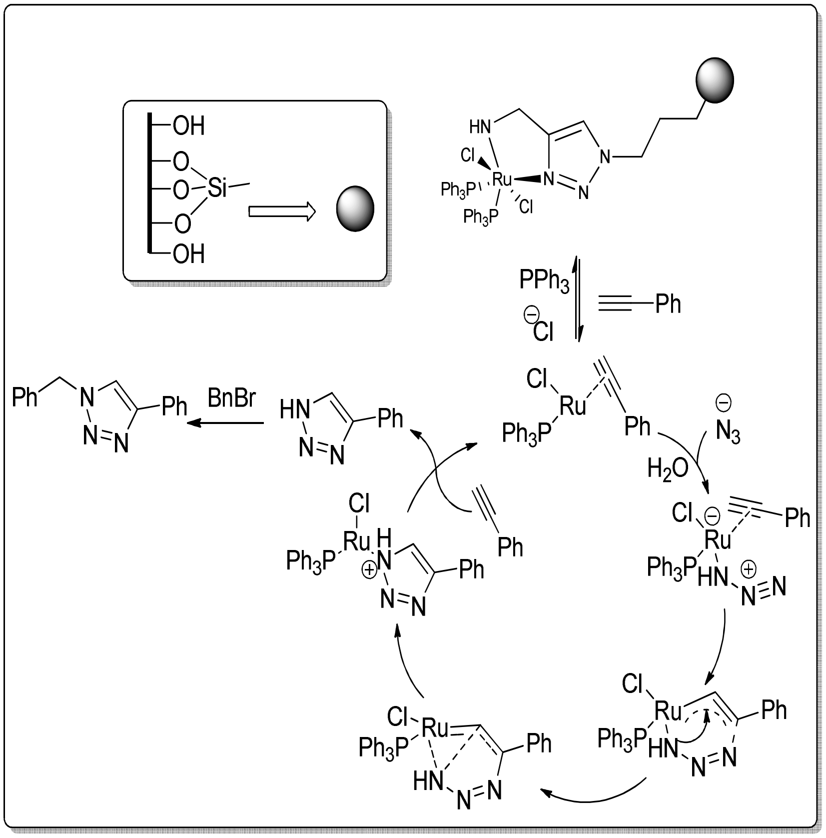

Figure 10. Plausible mechanism for the Multicomponant click reaction.

Lower temperature does not favor the formation of the product (1,4-disubstituted 1,2,3-triazole), however the yield of the triazole increased sharply up to 88% with an increase in the reaction temperature at 90°C for 12 h under optimized reaction conditions. It is noteworthy that the optimum reaction temperature with respect to conversion towards the triazole product, under the present reaction conditions, was found to be 90°C. To establish the proficiency in catalytic activity of synthesized heterogeneous SBA-15-Tz-Ru(II)TPP catalyst under optimized reaction conditions, a wide series of nonsubstituted and substituted phenyl acetylenes were allowed to react with benzyl halides and sodium azide to produce the corresponding triazole, in good to excellent yields (Table 4). The mono-substituted phenyl acetylenes afforded the product triazole in 88% yield (Table 4, entry 1). It is evident that the electron withdrawing or electron donating groups (EWG and EDG) attached to the phenyl acetylenes do not affect much the rate of reaction (Table 4 entries 2-10). In case of methyl (-CH_3) nitro (-NO_2) and –CN and -COMe substituted phenyl acetylene reacted smooothly and obtaind excellent yield of respective triazoles (Table 4 entries 2, 5, 3, 6). Similarly, the reaction with alkoxy substituted phenyl acetylene also furnished the corresponding product in good to excellent yield of product (Table 4 entries 4, 7, 8, 9). Interestingly, the bulky aromatic acetylenes also afforded the corresponding product in excellent yield (~89%) (Table 4, entry 10) (SI, S10, S11).

Though, the exact mechanism is not clearly understood at this point but to support the regioselective formation of 1,4-disubstituted 1,2,3-triazole product, a few controlled experiments were performed. In the present study, Ru-catalyzed multi-component reaction gives the exclusively the regioselective 1,4-disubstituted triazole compounds.[38] As our proposed method is multi-component, the opposite regioselectivity can be achieved; if the reaction sequence follows first the Ru-catalyzed cycloaddition of azide and alkyne to give the intermediate 4-phenyl-*1H*-1,2,3-triazole followed by sequential in situ substitution reaction with benzyl bromide to give the reported 1,4-disubstituted 1,2,3-triazole compounds (scheme 5a). To prove our hypothesis, first the reaction was carried out without benzyl bromide, which was completed within six hours furnishing the 4-phenyl-*1H*-1,2,3-triazole in excellent yield (83 %) under the optimized reaction conditions (NMR data are in good agreement with the literature report) (Scheme 5b) (See SI for NMR detail, S11). The isolated intermediate when subjected to substitution reaction with benzyl bromide under the similar reaction condition, it afforded expected 1,4-

View Article Online
DOI: 10.1039/C7CY02619F

disubstituted 1,2,3-triazole product (Scheme 5c). The same product was obtained even employing the homogeneous catalyst tris(triphenylphosphine)ruthenium(II) dichloride [$RuCl_2(PPh_3)_3$]. The plausible mechanism for the regio selectivity formation of 1,4-disubstituted triazole is given in figure 10.

Hydrogen Transfer Reaction

Generally, classical hydrogen transfer reaction needs dry organic solvent, inert atmosphere, prolonged reaction time period and homogeneous catalysts.[11a, 39]. Backvall *et al.* reported appreciable activity of various homogeneous ruthenium catalyzed hydrogen transfer reaction of different ketones.[40] In addition, few groups demonstrated potential of other metal complexes in homogeneous system for hydrogen transfer reactions. However, these catalytic systems face the drawbacks viz; tedious synthesis procedure, low TON, no recycling of expensive catalysts.[41] whereas the present developed protocol comprises benefits with minimal amount of catalyst, reuse and recycling of catalyst with high TON under ambient catalytic reaction conditions.

The synthesized heterogeneous SBA-15-Tz-Ru(II)TPP catalyst was investigated for hydrogen transfer reaction using cyclohexanone as a model substrate. Under the optimized reaction conditions the heterogeneous catalyst SBA-15-Tz-Ru(II)TPP (30 mg), isopropanol (10 mL), 2-cyclohexanone (2 mmol) and NaOH (0.5 mmol) was stirred at 80°C (Scheme 4). The progress of the reaction was monitored by GC. After the completion of reaction the usual workup gave the expected product in excellent yields.

To demonstrate the catalytic strength of SBA-15-Tz-Ru(II)TPP, a blank reaction was carried out without SBA-15-Tz-Ru(II)TPP catalyst and no product was detected in GC even after 24 h using isopropanol and cyclohexanone as a standard substrate under the optimised reaction conditions.

In order to further optimise the reaction conditions, various bases such as NEt_3, $NaHCO_3$, KOH, NaOH and K_2CO_3 were screened for the model reaction [Substrate isopropanol (10 mL) and cyclohexanone (2 mmol)]. The order of reactivity for the transfer hydrogenation reaction of the cyclohexanone in the presence of various bases could be arranged in following order NaOH (100%) > KOH (98%) > K_2CO_3 (50%) > $NaHCO_3$ (40%) ≫ NEt_3 (10%). NaOH was found to be the most suitable base for the reaction (Table 5).

A variety of carbonyl compounds were hydrogenated under transfer hydrogenation reaction conditions using different alcohols as hydrogen doner using SBA-15-Tz-Ru(II)TPP catalyst results are summerised in Table 6. Carbonyl compounds such as benzaldehyde, cyclohexanone, acetophenone, were hydrogenated smoothly using isopropanol to give the excellent yield of corresponding alcohols (Table 6, entries 1, 2, 3, 4). Further, the aldehyde with electron withdowing group such as 4-chloro and 4-nitrobenzaldehyde reacted at much faster rate irrespective of the hydrogen donor alcohols (primary, secondary, tertiary) furnishing the corresponding product in excellent yields and with high TON (Table 6, entries 5-10).

To study the heterogeneous nature and stability of synthesized SBA-15-Tz-Ru(II)TPP catalyst, Sheldon's hot filtration test was carried out showing that there is nearly no ruthenium leaching into the reaction solution during course of the reaction. To perform the Sheldon's hot filtration test for optimized reaction condition, catalyst SBA-15-Tz-Ru(II)TPP was filtered out from the reaction mixture after 1 h during the reaction, and the filtrate was again transfered into the RBF for further continuation of the reaction without catalyst. The GC analysis of filtrate was confirmed that conversation was up to 41% of corresponding product. As confirmed by GC analysis there was no improvement in the yield of hydrogen transferred product even prolongation of hot filtrate reaction for addtional 10 h. Similarly the hot filtration test of multicomponent click cycloaddition was also performed under optimized condition, SBA-15-Tz-Ru(II)TPP catalyst was filtered off from the reaction mixture after 2 h and the reaction continued uninterrupted in the absence of heterogeneous catalyst up to next 12 h. GC analysis showed that 20% conversion to the corresponding product after 2 h and the further conversion of multi component click cycloaddition remained constant up to 12 h. In both reactions, results show product formation more than 80% (ICP result, SI, S9).

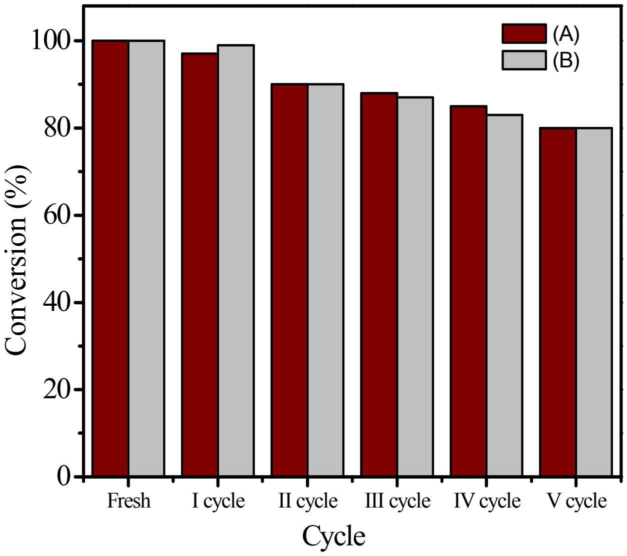

Figure 11. Recycle study of (A) hydrogen transfer reaction, (B) Multi component click cycloaddition.

Further, for the stability and recyclability study of the developed heterogeneous catalyst, SBA-15-Tz-Ru(II)TPP was recycled five times (fresh + four cycles) in both one pot multi component click cycloaddition, and in the hydrogen transfer reaction. After each cycle, the heterogeneous SBA-15-Tz-Ru(II)TPP catalyst was removed by simple centrifugation, washed several times with a suitable solvent dichloromethane or ethanol (10 mL at 80°C) and dried under oven overnight (Fig. 11). In every cycle, no considerable change was observed in the conversion and selectivity of the corresponding reaction product. Finally, after the last cycle, the ICP-OES analysis of the

View Article Online
DOI: 10.1039/C7CY02619F

used catalyst showed nearly stable ruthenium metal content with respect to the fresh catalyst (SI, S9). Conducted experiments confirm the heterogeneous nature of SBA-15-Tz-Ru(II)TPP and stability which could be retained up to the several cycle of the reactions.

Conclusions

In summary, we demonstrated an efficient method for ligand synthesis and covalent tethering to solid support, in a single step using "click chemistry". A new highly efficient, heterogeneous SBA-15-Tz-Ru(II)TPP catalyst is developed by immobilizing $[RuCl_2(PPh_3)_3]$ complex over triazole functionalized SBA-15. The catalytic efficiency of SBA-15-Tz-Ru(II)TPP was established for multicomponent click cycloaddition and hydrogen transfer reaction. Surprisingly, multi-component cycloaddition reaction exhibit remarkable reactivity in water medium for the regioselective synthesis of 1,4-disubstituted 1,2,3-triazole in excellent yields in contrast to the literature report of 1,5-disubstituted 1,2,3-triazole formation. Additionally, in hydrogen transfer reactions, screened carbonyl compounds, shows up to 100% conversion to give hydrogen transferred products. The salient features of the heterogeneous catalyst SBA-15-Tz-Ru(II)TPP are its stability in water as reaction medium, heterogeneous nature and recyclability without loss of activity.

B Synthetic procedures, Materials and methods, Crystallography.

Experimental

The materials used, such as Pluronic 123 (P123, average Mol.Wt. = 5800), tetraethylorthosilicate (TEOS), 3-aminopropyltrimethoxysilane (3-APTMS), $[RuCl_2(PPh_3)_3]$, sodium azide (NaN_3), *N*, *N*-diisopropylethylamine (DIPEA), copper iodide (CuI), propargylamine, aldehyde, alcohols were purchased from Aldrich. Furthermore, solvents like dichloromethane (DCM), tetrahydrofuran (THF), acetonitrile (CH_3CN) and toluene were purchased from Merck.

Synthesis of heterogeneous catalyst SBA-15-Tz-Ru(II)TPP:

The synthesis of SBA-15 was carried out by following the well established modified literature procedure [27a, 28a, 29] with the following initial molar compositions, (180.043) TEOS: 4.4 g P_{123} Mavg = 5800 $[EO_{20}–PO_{70}–EO_{20}]$: (8.33) H_2O: (0.24) HCl, Pluronic 123 called as P_{123} (4.4 g), a triblock co-polymer (surfactant), was dispersed in 30 g distilled water and stirred for 1.5 h. 120 g of 2M HCl added into the solution with constant stirring and continued for further 2 h. At the same time, 9 g of TEOS (precursor) was added drop wise and resulting solution was maintained at 35°C for next 24 h with stirring. The mixture was kept for hydrothermal treatment at 100°C for 48 h under static conditions. The obtained material was filtered, washed with distilled water and dried in oven at 70°C for 12 h, and later calcined at 540°C for 8 h in air to get calcined SBA-15 (11.5 g).

Surface modification over SBA-15 via azide group

SBA-15 was modified with 3-azidopropyltrimethoxysilane (Az-PTMS) via post grafting method.[8, 30a] In 1 g SBA-15 mixture with 50 mL toluene, 3.5 mL 3-azidopropyl trimethoxysilane (Az-PTMS) was added. The resulting mixture was stirred for 12 h at 90ºC in inert atmosphere. After completion of reaction, the solid was filtered and washed with toluene to remove unreacted 3-Az-PTMS, further dried at 60°C for 12 h in oven to get SBA-15-N_3. Yield: 1.20 g (solid) and preserved under inert atmosphere (Scheme 1B).

Ligand formation by using SBA-15-N_3 and propargylamine (Via click)

Triazole ligand formation over clickable SBA-15 surface was accomplished by following a method described in an earlier report from our group.[8] In a 25 mL round bottom flask with a magnetic stir bar, copper(I) iodide (0.5 mg) and vacuum distilled N,N-diisopropylethylamine (DIPEA) (1 mL) were charged with anhydrous, nitrogen-purged dimethylformamide (DMF) (3 mL). The reaction mixture was stirred (till the solution turned green) and in further step, transferred to tetrahydrofuran (THF) reaction mixture (7.5 mL) containing 3-azidopropyltrimethoxysilane (Az-PTMS) modified mesoporous SBA-15 (SBA-15-N_3) (0.5 g). Further, the propargylamine (10 mmol) were added and stirred at 50°C for 12 h. The modified material was ultrasonicated for 20 min, washed with THF, and dried under inert atmosphere. The material was kept in desiccators in absence of light for further characterization and modification (Scheme 1C). The obtained material is abbreviated as SBA-15-Tz (yield 0.75 g).

SBA-15-Tz anchoring by tris(triphenylphosphine)ruthenium(II) dichloride $[RuCl_2(PPh_3)_3]$ complex

Modified SBA-15 material (SBA-15-Tz) (1 g) was added to the solution of $[RuCl_2(PPh_3)_3]$ (0.15 mmol) in DMF (50 mL) and refluxed under argon for 12 h. Later, the product was allowed to cool and filtered. The obtained gray color solid was washed with THF (25 mL) and acetone (25 mL). Further, product was soxhlet extracted with dichloromethane (CH_2Cl_2) for 24 h to remove unreacted $[RuCl_2(PPh_3)_3]$ and organic impurities (Scheme 1D). The resulting product was dried with the help of vacuum at 75°C to furnish 1.4 g of the SBA-15-Tz-Ru(II)TPP.

Multi Component Click reaction

In the 50 mL round bottom flask, alkyne (1 mmol), sodium azide (1.2 mmol), benzyl bromide (1.2 mmol) and SBA-15-Tz-Ru(II)TPP catalyst 15 mg were taken followed by addition of 3 ml of water as solvent. The mixture was stirred at 90°C in the preheated oil bath for given time. Progress of the reaction was monitored by TLC (2:8 ethyl acetate: pet ether). After the completion of reaction, 10 mL of ethyl acetate added to the reaction mixture and filtered to recover the SBA-15-Tz-Ru(II)TPP catalyst. Residue was washed with ethyl acetate (5 mL x 3 times). Combined organic layer was dried with anhydrous sodium sulphate and concentrated under the reduced pressure. The crude product was purified by the

View Article Online
DOI: 10.1039/C7CY02619F

column chromatography to get the product 4 a-n (Scheme 3). The product was characterized by GCMS and ^{1}H & ^{13}C NMR analysis (SI, S10, S11).

Hydrogen Transfer Reaction

In a 25 mL two neck round bottom flask, carbonyl compounds (2 mmol), NaOH (0.5 mmol), alcohol (isopropanol) (10 mL), and SBA-15-Tz-Ru(II)TPP catalyst (30 mg) were stirred under argon at 80°C. The reaction mixture was analyzed by GC at measured time intervals (Scheme 4).

Results and Discussion

Characterization

Powder X-ray diffraction (XRD) patterns were measured on a PAN analytical X’pert Pro dual goniometer diffractometer using Ni-filtered CuKa radiation (l = 1.5404 Å) over the range 0.5–51 (SAXRD). N_2 adsorption–desorption isotherms, pore size distributions as well as the textural properties of the hybrid materials were determined by using a Autosorb 1C Quantachrome USA. The program consisting of both an adsorption and desorption branch typically ran at -196°C after samples were degassed at 150°C for 4 h. The BET method was applied to calculate the total surface area at relative pressures of P/P_0 = 0.65–0.45 and the BJH model was applied to the adsorption branch of the isotherm to determine the total pore volume and average pore diameter at a relative pressure of P/P_0 = 0.99. Pore size distribution curves were obtained via the NLDFT model assuming cylindrical pore geometry. Magic angle spinning (MAS) NMR spectra of ^{29}Si, ^{31}P and ^{13}C nuclei were recorded on a BRUKER DSX300 spectrometer at 7.05 T (resonance frequencies 59.595 MHz, rotor speed 10 000 Hz and 75.43 MHz, rotor speed 10 000 Hz). XPS analysis was conducted using XPS Kratos AXIs Ultra (Kratos Analytical Ltd., UK) high resolution photoelectron spectroscopy instrument. FTIR spectra were recorded on a Bruker Alpha-T. Sample morphology was observed by extra High-Resolution Scanning Electron Microscopy (MagellanTM 400 L). Thermal analysis (TGA) of the samples was conducted using a Pyris Diamond TGA analyzer with a heating rate of 100ºC min^{-1} under air atmosphere. GC analyses were performed using Focus GC from Thermo Electron Corporation, equipped with low polarity ZB-5 column. GC analyses were performed using Trace 1300 Gas Chromatograph model from Thermo Scientific, equipped with the Rxi-1ms (crossbond 100% dimethyl polysiloxane) column. Conversion based on GC area. The ruthenium (Ru) content of product was determined by an Inductively Coupled Plasma Mass Spectrometry (ICPMS) spectrometer (Agilent 7500 cx).

Conflicts of interest

“There are no conflicts to declare”.

Acknowledgements

The APS acknowledges CSIR, New Delhi for the financial support in the form of an Emeritus Scientist project (P81103). PK is grateful to INSA, New Delhi for financial support under senior scientist program. Jayant Rathod thanks the Council of Scientific and Industrial Research (CSIR), New Delhi for a Senior Research Fellowship. P. Sharma gratefully acknowledges the project (Grant No. 207/12 Israel grant) for financial support.

Notes and references

1 a)H. C. Kolb, K. B. Sharpless, *Drug Discov. Today* **2003**, *8*, 1128-1137; b)D. Dheer, V. Singh, R. Shankar, *Bioorganic Chemistry* **2017**, *71*, 30-54.
2 J.-F. Lutz, Z. Zarafshani, *Adv. Drug Deliv. Rev.* **2008**, *60*, 958-970.
3 a)R. Huisgen, G. Szeimies, L. Möbius, *Chem. Ber.* **1967**, *100*, 2494-2507; b)M. S. Singh, S. Chowdhury, S. Koley, *Tetrahedron* **2016**, *72*, 5257-5283.
4 a)H. Struthers, T. L. Mindt, R. Schibli, *Dalton Trans.* **2010**, *39*, 675-696; b)T. Romero, R. A. Orenes, A. Espinosa, A. Tárraga, P. Molina, *Inorg. Chem.* **2011**, *50*, 8214-8224; c)J. P. Byrne, J. A. Kitchen, T. Gunnlaugsson, *Chem. Soc. Rev.* **2014**, *43*, 5302-5325.
5 R. M. Meudtner, M. Ostermeier, R. Goddard, C. Limberg, S. Hecht, *Chem. – Eur. J.* **2007**, *13*, 9834-9840.
6 a)D. Schweinfurth, R. Pattacini, S. Strobel, B. Sarkar, *Dalton Trans.* **2009**, 9291-9297; b)D. Schweinfurth, C.-Y. Su, S.-C. Wei, P. Braunstein, B. Sarkar, *Dalton Trans.* **2012**, *41*, 12984-12990.
7 J. D. Crowley, D. A. McMorran, in *Click Triazoles* (Ed.: J. Košmrlj), Springer Berlin Heidelberg, Berlin, Heidelberg, **2012**, pp. 31-83.
8 P. Sharma, A. P. Singh, *RSC Adv.* **2014**, *4*, 43070-43079.
9 S.-H. Cho, T. Gadzikwa, M. Afshari, S. T. Nguyen, J. T. Hupp, *Eur. J. Inorg. Chem.* **2007**, *2007*, 4863-4867.
10 a)C. T. Kresge, M. E. Leonowicz, W. J. Roth, J. C. Vartuli, J. S. Beck, *Nature* **1992**, *359*, 710-712; b)J. S. Beck, J. C. Vartuli, W. J. Roth, M. E. Leonowicz, C. T. Kresge, K. D. Schmitt, C. T. W. Chu, D. H. Olson, E. W. Sheppard, S. B. McCullen, J. B. Higgins, J. L. Schlenker, *J. Am. Chem. Soc.* **1992**, *114*, 10834-10843.
11 a)R. D. Patil, Y. Sasson, *Asian J. Org. Chem.* **2015**, *4*, 1258-1261; b)S.-Q. Bai, L. Jiang, J.-L. Zuo, T. S. A. Hor, *Dalton Trans.* **2013**, *42*, 11319-11326; c)Z. Gonda, Z. Novak, *Dalton Trans.* **2010**, *39*, 726-729; d)D. Wang, M. Zhao, X. Liu, Y. Chen, N. Li, B. Chen, *Org. Biomol. Chem.* **2012**, *10*, 229-231; e)F. Wang, H. Fu, Y. Jiang, Y. Zhao, *Green Chem.* **2008**, *10*, 452-456.
12 a)L. Jiang, Z. Wang, S.-Q. Bai, T. S. A. Hor, *Dalton Trans.* **2013**, *42*, 9437-9443; b)F. Nador, M. A. Volpe, F. Alonso, A. Feldhoff, A. Kirschning, G. Radivoy, *Appl. Catal. A.* **2013**, *455*, 39-45.
13 a)M. Singla, P. Mathur, M. Gupta, M. S. Hundal, *Transition Met. Chem.* **2008**, *33*, 175-182; b)K. R. Gruenwald, A. M. Kirillov, M. Haukka, J. Sanchiz, A. J. L. Pombeiro, *Dalton Trans.* **2009**, *12*, 2109-2120.

View Article Online
DOI: 10.1039/C7CY02619F

14 a)C. Wang, D. Ikhlef, S. Kahlal, J.-Y. Saillard, D. Astruc, *Coordination Chemistry Reviews* **2016**, *316*, 1-20; b)A. Tăbăcaru, B. Furdui, I. O. Ghinea, G. Cârâc, R. M. Dinică, *Inorganica Chimica Acta* **2017**, *455*, 329-349.

15 J. R. Johansson, T. Beke-Somfai, A. Said Stålsmeden, N. Kann, *Chemical Reviews* **2016**, *116*, 14726-14768.

16 a)B. C. Boren, S. Narayan, L. K. Rasmussen, L. Zhang, H. Zhao, Z. Lin, G. Jia, V. V. Fokin, *J. Am. Chem. Soc.* **2008**, *130*, 8923-8930; b)S. Oppilliart, G. Mousseau, L. Zhang, G. Jia, P. Thuéry, B. Rousseau, J.-C. Cintrat, *Tetrahedron* **2007**, *63*, 8094-8098; c)M. M. Majireck, S. M. Weinreb, *J. Org. Chem.* **2006**, *71*, 8680-8683; d)Y.-H. Lo, T.-H. Wang, C.-Y. Lee, Y.-H. Feng, *Organometallics* **2012**, *31*, 6887-6899; e)D.-R. Hou, T.-C. Kuan, Y.-K. Li, R. Lee, K.-W. Huang, *Tetrahedron* **2010**, *66*, 9415-9420.

17 P. N. Liu, J. Li, F. H. Su, K. D. Ju, L. Zhang, C. Shi, H. H. Y. Sung, I. D. Williams, V. V. Fokin, Z. Lin, G. Jia, *Organometallics* **2012**, *31*, 4904-4915.

18 a)J.-E. Bäckvall, *J. Organomet. Chem.* **2002**, *652*, 105-111; b)X. Wu, J. Xiao, *Chem.Commun.* **2007**, *24*, 2449-2466; c)S. E. Clapham, A. Hadzovic, R. H. Morris, *Coord. Chem. Rev.* **2004**, *248*, 2201-2237; d)P. Albin, J. Blum, E. Dunkelblum, Y. Sasson, *J Org. Chem.* **1975**, *40*, 2402-2403.

19 a)G. Brieger, T. J. Nestrick, *Chem. Rev.* **1974**, *74*, 567-580; b)R. A. W. Johnstone, A. H. Wilby, I. D. Entwistle, *Chem. Rev.* **1985**, *85*, 129-170; c)P. K. Mandal, J. S. McMurray, *J Org Chem.* **2007**, *72*, 6599-6601.

20 R. Tao, Y. Xie, G. An, K. Ding, H. Zhang, Z. Sun, Z. Liu, *J. Colloid. Interface Sci.* **2010**, *351*, 501-506.

21 S. U. Sonavane, R. V. Jayaram, *Synth. Commun.* **2003**, *33*, 843-849.

22 L. He, J. Ni, L.-C. Wang, F.-J. Yu, Y. Cao, H.-Y. He, K.-N. Fan, *Chem. – Eur. J* **2009**, *15*, 11833-11836.

23 a)X. Wu, J. Liu, X. Li, A. Zanotti-Gerosa, F. Hancock, D. Vinci, J. Ruan, J. Xiao, *Angew. Chem., Int. Ed.* **2006**, *45*, 6718-6722; b)A. Bényei, F. Joó, *J Mol. Catal. A Chem.* **1990**, *58*, 151-163.

24 a)T. Ikariya, A. J. Blacker, *Acc. Chem. Res.* **2007**, *40*, 1300-1308; b)F.-Z. Su, L. He, J. Ni, Y. Cao, H.-Y. He, K.-N. Fan, *Chem.Commun.* **2008**, *30*, 3531-3533.

25 a)W. Ye, M. Zhao, W. Du, Q. Jiang, K. Wu, P. Wu, Z. Yu, *Chem. – Eur. J* **2011**, *17*, 4737-4741; b)J. Toubiana, Y. Sasson, *Catal. Sci. Technol.* **2012**, *2*, 1644-1653.

26 a)W. Ye, M. Zhao, Z. Yu, *Chem. – Eur. J* **2012**, *18*, 10843-10846; b)S. Gladiali, E. Alberico, *Chem. Soc. Rev.* **2006**, *35*, 226-236.

27 a)P. Sharma, A. P. Singh, *RSC Adv.* **2014**, *4*, 58467-58475; b)A. Lazar, W. R. Thiel, A. P. Singh, *RSC Adv.* **2014**, *4*, 14063-14073.

28 a)A. Lazar, C. P. Vinod, A. P. Singh, *New J. Chem.* **2016**, *40*, 2423-2432; b)D. Zhao, J. Feng, Q. Huo, N. Melosh, G. H. Fredrickson, B. F. Chmelka, G. D. Stucky, *Science* **1998**, *279*, 548-552.

29 A. Lazar, P. Sharma, A. P. Singh, *Micropor. Mesopor. Mat.* **2013**, *170*, 331-339.

30 a)M. Kar, B. Malvi, A. Das, S. Panneri, S. S. Gupta, *J. Mater. Chem.* **2011**, *21*, 6690-6697; b)B. Malvi, B. R. Sarkar, D. Pati, R. Mathew, T. G. Ajithkumar, S. Sen Gupta, *J. Mater. Chem.* **2009**, *19*, 1409-1416; c)J. Gao, X. Zhang, S. Xu, J. Liu, F. Tan, X. Li, Z. Qu, Y. Zhang, X. Quan, *Chem. Asian J.* **2014**, *9*, 908-914.

31 a)A. Ghosh, R. Kumar, *Micropor. Mesopor. Mat.* **2005**, *87*, 33-44; b)T. Joseph, S. S. Deshpande, S. B. Halligudi, A. Vinu, S. Ernst, M. Hartmann, *J. Mol. Catal. A: Chem.* **2003**, *206*, 13-21.

32 S. Sisodiya, A. Lazar, S. Shylesh, L. Wang, W. R. Thiel, A. P. Singh, *Chem. Commun.* **2012**, *25*, 22-27.

33 S. Farsadpour, L. T. Ghoochany, S. Shylesh, G. Dörr, A. Seifert, S. Ernst, W. R. Thiel, *ChemCatChem* **2012**, *4*, 401-407.

34 a)A. Jana, J. Mondal, P. Borah, S. Mondal, A. Bhaumik, Y. Zhao, *Chem. Commun.* **2015**, *51*, 10746-10749; b)C. Agnes, J.-C. Arnault, F. Omnes, B. Jousselme, M. Billon, G. Bidan, P. Mailley, *Phys. Chem. Chem. Phys.* **2009**, *11*, 11647-11654.

35 a)B. Dervaux, F. E. Du Prez, *Chem. Sci.* **2012**, *3*, 959-966; b)V. Bénéteau, A. Olmos, T. Boningari, J. Sommer, P. Pale, *Tetrahedron Lett.* **2010**, *51*, 3673-3677; c)E. Ozkal, S. Ozcubukcu, C. Jimeno, M. A. Pericas, *Catal. Sci. Technol.* **2012**, *2*, 195-200.

36 a)B. H. Lipshutz, B. R. Taft, *Angew. Chem.* **2006**, *118*, 8415-8418; b)M. Nasr-Esfahani, I. Mohammadpoor-Baltork, A. R. Khosropour, M. Moghadam, V. Mirkhani, S. Tangestaninejad, H. Amiri Rudbari, *J. Org. Chem.* **2014**, *79*, 1437-1443.

37 a)H. Sharghi, M. H. Beyzavi, A. Safavi, M. M. Doroodmand, R. Khalifeh, *Adv. Synth. Catal.* **2009**, *351*, 2391-2410; b)H. Sharghi, R. Khalifeh, M. M. Doroodmand, *Adv. Synth. Catal.* **2009**, *351*, 207-218.

38 B. C. Boren, S. Narayan, L. K. Rasmussen, L. Zhang, H. Zhao, Z. Lin, G. Jia, V. V. Fokin, *Journal of the American Chemical Society* **2008**, *130*, 8923-8930.

39 a)A. Aranyos, G. Csjernyik, K. J. Szabo, J.-E. Backvall, *Chem. Commun.* **1999**, 351-352; b)R. L. Chowdhury, J.-E. Backvall, *Chem. Commun.* **1991**, 1063-1064; c)S. Mazza, R. Scopelliti, X. Hu, *Organometallics* **2015**, *34*, 1538-1545.

40 a)G. Z. Wang, J.-E. Backvall, *Chem. Commun.* **1992**, 337-339; b)Y. R. S. Laxmi, J.-E. Backvall, *Chem. Commun.* **2000**, 611-612.

41 a)R. Langer, G. Leitus, Y. Ben-David, D. Milstein, *Angew. Chem. Int. Ed.* **2011**, *50*, 2120-2124; b)A. Mikhailine, A. J. Lough, R. H. Morris, *J. Am. Chem. Soc.* **2009**, *131*, 1394-1395.

View Article Online
DOI: 10.1039/C7CY02619F

Table 2. Optimization for multi component cycloaddition reaction in homogeneous and heterogeneous medium.

S.No.	Catalyst	Ligand	Solvent	Yield (%)
1.	$RuCl_3$	PPh_3	DMF	6
2.	$RuCl_3$	PPh_3	DMSO	24
3.	$RuCl_3$	PPh_3	Dioxane	26
4.	$RuCl_3$	PPh_3	Toluene	5
5.	$RuCl_3$	PPh_3	Water	48
6.	$RuCl_3$	DMAP	Water	32
7.	$RuCl_3$	2-amino-6-picoline	Water	10
8.	$[Ru(p\text{-}cym)Cl]_2$	--	Water	26
9.	SBA-15-Tz-u(II)TPP	--	Water	88

Reaction conditions: Phenyl acetylene (1 mmol), Benzyl bromide (1.2 mmol), Sodium azide (1.2 mmol), Catalyst (Ruthenium 0.445 mol %) and solvent (3 mL).

Table 3. Solvent optimization for multi component cycloaddition reaction.

Entry	Solvent	Time (h)	Temperature (°C)	Yield (%)
1.	DMSO	24	RT	00
2.	DMSO	12	90	46
3.	DMF	12	90	63
4.	t-BuOH	12	90	35
5.	EtOH	24	90	50
6.	**H_2O**	**12**	**90**	**88**
7.	H_2O	24	RT	00
8.	THF	12	90	20

Reaction conditions: Phenyl acetylene (1 mmol), Benzyl bromide (1.2 mmol), Sodium azide (1.2 mmol), SBA-15-Tz-Ru(II)TPP Catalyst (15 mg, Ruthenium metal 0.445 mol %) and solvent (3 mL).

Table 4: Multi component click cycloaddition using SBA-15-Tz-Ru(II)TPP.

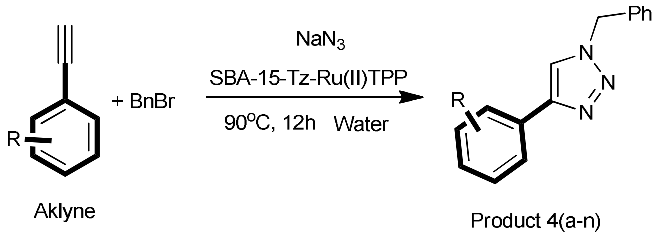

View Article Online
DOI: 10.1039/C7CY02619F

S.No.	Alkynes	Product	Yields (%)[a]	Entry
1.	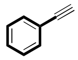	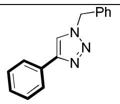	88	4a
2.	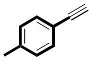	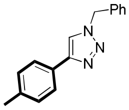	86	4b
3.	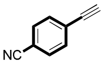	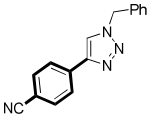	92	4c
4.	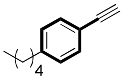	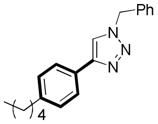	78	4d
5.	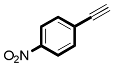	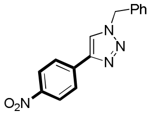	82	4e
6.	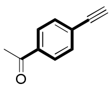	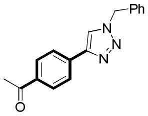	77	4f
7.	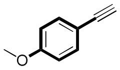	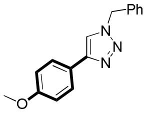	86	4g
8.	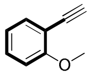	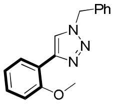	70	4h
9.	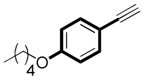	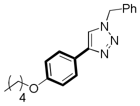	76	4i
10.	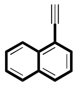	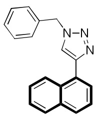	89	4j
11.	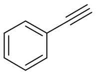	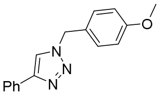	87[b]	4k
12.	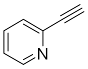	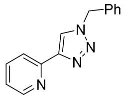	85	4l
13.		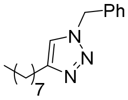	73[c]	4m
14.	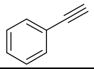	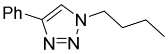	76[d]	4n

Reaction Conditions: Phenyl acetylene (1 mmol), Benzyl bromide (1.2 mmol), Sodium azide (1.2 mmol), Catalyst SBA-15-Tz-Ru(II)TPP (15 mg, Ruthenium metal 0.445 mol %) and solvent (3 mL), time period 12 h. a) Isolated Yields, b) PMB-Cl was used in place of BnBr, c) 1-decyne as alkyne, d) 1-Bromobutane was used in place of BnBr.

View Article Online
DOI: 10.1039/C7CY02619F

Table 5: Base optimization for catalytic hydrogen transfer reaction.

S.No.	Base	Yield (%)
1.	NaOH	100
2.	KOH	98
3.	K_2CO_3	50
4.	$NaHCO_3$	40
5.	NEt_3	10

Reaction conditions: SBA-15-Tz-Ru(II)TPP (30 mg, Ruthenium metal 0.445 mol %), Alcohol (10 mL), carbonyl compound (2 mmol), base (0.5 mmol), 80°C Isolated yields; Product analyzed by GC. Conversion based on GC area.

Table 6: Catalytic hydrogen transfer reaction using SBA-15-Tz-Ru(II)TPP catalyst.

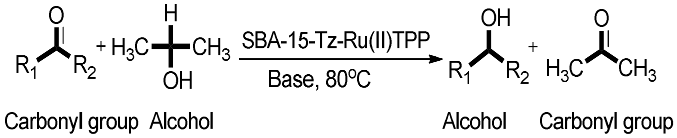

View Article Online
DOI: 10.1039/C7CY02619F

S.No.	Carbonyl compound	Alcohol	Product	Time (h)	Yield (%)	TON
1.	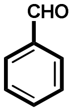	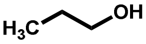	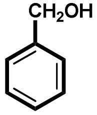	6	89	200
2.	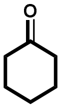	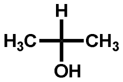	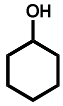	6	71	160
3.	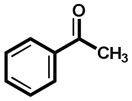	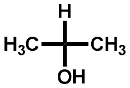	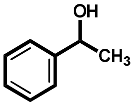	6	73	164
4.	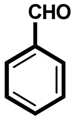	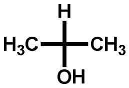	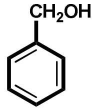	6	80	180
5.	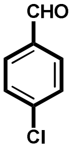	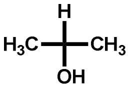	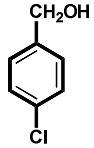	2	92	207
6.	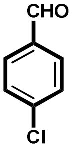	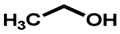	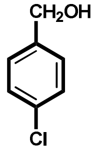	2	97	218
7.	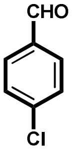	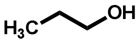	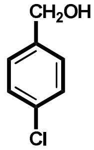	2	85	191
8.	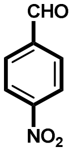	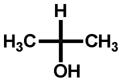	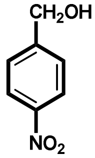	1	95	213
9.		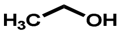	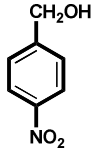	1.5	99	223
10.	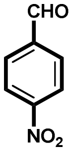	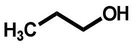	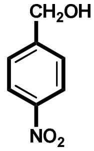	2	80	180

Reaction conditions: SBA-15-Tz-Ru(II)TPP (30 mg, Ruthenium metal 0.445 mol %), Alcohol (10 mL), carbonyl compound (2 mmol), NaOH (0.5 mmol), 80°C Isolated yields; Product analyzed by GC. Conversion and yield based on GC area.

View Article Online
DOI: 10.1039/C7CY02619F

Table of Content

Synthesis of Heterogeneous Ru(II)-1,2,3-Triazole catalyst supported over SBA-15: Application to the Transfer Hydrogen reaction and unusual highly selective 1,4-disbustituted traizole formation via Multicomponent Click Reaction

Priti Sharma#[a], Jayant Rathod#[c], A.P. Singh*[b], Pradeep Kumar*[c] and Yoel Sasson*[a]